Nat. Hazards Earth Syst. Sci., 11, 2803–2816, 2011
www.nat-hazards-earth-syst-sci.net/11/2803/2011/
doi:10.5194/nhess-11-2803-2011

Natural Hazards and Earth System Sciences

Impact of the use of a CO_2 responsive land surface model in simulating the effect of climate change on the hydrology of French Mediterranean basins

S. Queguiner[1], E. Martin[1], S. Lafont[1], J.-C. Calvet[1], S. Faroux[1], and P. Quintana-Seguí[2]

[1]CNRM/GAME (Météo-France, CNRS), URA 1357, Toulouse, France
[2]Observatori de l'Ebre, Universitat Ramon Llull – CSIC, Roquetes, Spain

Received: 27 October 2010 – Revised: 29 August 2011 – Accepted: 15 September 2011 – Published: 24 October 2011

Abstract. In order to evaluate the uncertainty associated with the impact model in climate change studies, a CO_2 responsive version of the land surface model ISBA (ISBA-A-gs) is compared with its standard version in a climate impact assessment study. The study is performed over the French Mediterranean basin using the Safran-Isba-Modcou chain. A downscaled A2 regional climate scenario is used to force both versions of ISBA, and the results of the two land surface models are compared for the present climate and for that at the end of the century. Reasonable agreement is found between models and with discharge observations. However, ISBA-A-gs has a lower mean evapotranspiration and a higher discharge than ISBA-Standard. Results for the impact of climate change are coherent on a yearly basis for evapotranspiration, total runoff, and discharge. However, the two versions of ISBA present contrasting seasonal variations. ISBA-A-gs develops a different vegetation cycle. The growth of the vegetation begins earlier and reaches a slightly lower maximum than in the present climate. This maximum is followed by a rapid decrease in summertime. In consequence, the springtime evapotranspiration is significantly increased when compared to ISBA-Standard, while the autumn evapotranspiration is lower. On average, discharge changes are more significant at the regional scale with ISBA-A-gs.

1 Introduction

The Mediterranean basin is recognized as an area particularly vulnerable to climate change during the 21st century. A pronounced decrease in precipitation, especially in the dry season, and an increase in temperature are expected, together with an increase in the climate variability (Giorgi, 2006; Giorgi and Lionello, 2008). In France, Boé et al. (2009) used an ensemble of climate scenarios to force the hydrometeorological model chain Safran-Isba-Modcou (SIM, Habets et al., 2008) over France and found a significant impact on the snow cover, surface water balance, and river flows, especially in the Mediterranean area.

Impact studies are usually designed as follows: global socioeconomic assumptions are made that are used to drive general circulation models (GCM); then the model results are downscaled and/or unbiased and used to force an impact model. The associated cascade of uncertainty in climate impact assessment begins with the construction of future emission scenarios and ends in impact assessment. In the past, significant attention has been paid to uncertainty in GCMs and emission scenarios. Recently, the role of the downscaling procedures has been studied in more detail. Leander et al. (2008) and van Pelt et al. (2009) showed that dynamical downscaling must be complemented by bias corrections or resampling in order to force hydrological models in climate change impact studies. Boé et al. (2009) compared a statistical downscaling method with a dynamical downscaling associated with a bias correction in a study at the scale of France, and concluded that the uncertainty associated with the downscaling method was not negligible but was lower than the uncertainty associated with GCMs. Quintana-Seguí et al. (2010), in a study of the Mediterranean area, compared three downscaling methods: dynamical, including bias correction; statistical; and the very simple anomaly method. They confirmed this result but found that the uncertainty in the downscaling could lead to significant differences when studying extreme rainfall or discharge events. The last two studies used the ISBA-MODCOU hydrometeorological model (Habets et al., 2008) in their hydrological impact assessment and did not treat the uncertainty associated with the hydrometeorological model.

Correspondence to: E. Martin
(eric.martin@meteo.fr)

Published by Copernicus Publications on behalf of the European Geosciences Union.

To date, little recognition has been given to the role of the hydrological model uncertainty in future assessments. The recent RexHySS (Ressources en eau et Extrêmes Hydrologiques dans les bassins de la Seine et la Somme) project (Ducharne et al., 2010) tried to compare the uncertainties associated with the socioeconomic scenario, the general circulation model, the time horizon, the downscaling method, and the hydrological model in a study of the Seine and Somme rivers in northern France. This study was done by multiplying the simulations using different socioeconomic scenarios (A2, A1B, B1) and using GCM results from the CMIP3 database for the middle and end of the 21st century. In addition, this study used two downscaling methods (Boé et al., 2009 and Déqué et al., 2007). The uncertainty associated with the hydrological model was assessed using five hydrological models. A robust decrease in summer flow was found, while moderate changes occurred in the flood regime. The major source of uncertainty came from the GCM, followed closely by the hydrological model and the downscaling method. This study, among the most comprehensive studies in the treatment of uncertainties, confirmed that the uncertainty associated with the hydrological model is not negligible in climate impact studies.

While the atmospheric carbon dioxide concentration is expected to increase significantly, most evapotranspiration formulations in hydrological models do not take into account the direct effect of carbon dioxide on plant physiology. Hence, the estimated evapotranspiration may be biased for future climate simulations. Actually, the increase in the atmospheric CO_2 concentration has a fertilization effect that leads to an increase in vegetation biomass and an antitranspirant effect that reduces the leaf stomatal conductance. The balance between the two effects depends on the climate and the type of plant. A comprehensive carbon cycle is introduced in some GCMs (e.g. Friedlingstein et al., 2006). At the global scale in offline mode, Gedney et al. (2006) considered only the antitranspirant effect and logically concluded that this effect may have contributed to an enhancement of river flows during the 20th century. Calvet et al. (2008) performed a sensitivity study with the ISBA-A-gs model, accounting for both fertilization and antitranspirant effects, for three vegetation types in southwestern France. A significant CO_2-driven reduction of canopy conductance was simulated for irrigated maize and coniferous forest, while the wheat response was more balanced.

In the present study, our objective is to contribute to the exploration of the uncertainty associated with the representation of land surface processes in climate impact studies. We focus on the Mediterranean area and compare two versions of the land surface model ISBA: the classical version of the land surface model ISBA (ISBA-Standard, Noilhan and Planton, 1989) and the more advanced version (ISBA-A-gs, Calvet et al., 1998) that takes into account the direct effect of carbon dioxide on plant physiology and explicitly simulates the combined impact on hydrology of changes in the water and carbon cycle. These models are described in detail in Sect. 3. The downscaled A2 climate scenario from Quintana-Seguí et al. (2010), covering the French Mediterranean described in Sect. 4, was used in this study. Then the two ISBA versions are compared and the impact on the simulated hydrological cycle is discussed.

2 The study area

This study was focused on the Mediterranean region of France, defined by the French Mediterranean basin (Fig. 1), with a surface of 147 000 km^2. The largest river is the Rhône. The corresponding basin covers a significant part of the region, encompassing a large range of climatic conditions (continental, Mediterranean, and Alpine climates). Some tributaries (e.g. the Isère and the Durance) are influenced by the snow cover, while the Saône river in the north of the domain is not subject to a Mediterranean climate but to an Atlantic influence. The area is also characterized by many small basins that flow directly to the Mediterranean or are tributaries of the Rhône in its southern part. The surface of the Rhône basin (including its Swiss part) is 95 500 km^2, while the surface of the other main Mediterranean rivers, such as the Aude, Hérault, Gardon, Ardèche, Huveaune and Var, varies from 373 to 6074 km^2.

Within this domain, a specific sub-domain consisting of the low lying areas with a dry Mediterranean climate was defined. The northern limit of the domain was fixed at 45° N (the limit commonly accepted for the Mediterranean climate in this region) and the altitude was limited to 1000 m a.s.l to avoid areas with significant snow cover (less than one month below 1000 m a.s.l.). This sub-domain is called "MedDom" (Mediterranean domain) hereafter. The surface of MedDom is 60 000 km^2, around 40 % of the original domain, hereafter called "FullDom". The delineation of MedDom can be seen in Fig. 1.

The climate characteristics of the area have been described by Quintana-Seguí et al. (2010). The mean annual temperature is around 15 °C near the coast, decreases to 10 °C in the north, and is much lower in mountainous areas. The mean annual precipitation does not exceed 510 mm yr^{-1} near the coast and increases with altitude. Maxima can be seen in the northern part of the French Alps, in the Jura mountains, and the Cévennes. Precipitation in the Cévennes is mainly due to Mediterranean storms affecting the region from September to December.

3 The hydrometeorological model

The hydrometeorological model used in this study is derived from the SIM chain of models described in Habets et al. (2008). It is composed of the coupling of the ISBA surface scheme (Interaction surface-biosphère-atmosphère, Noilhan

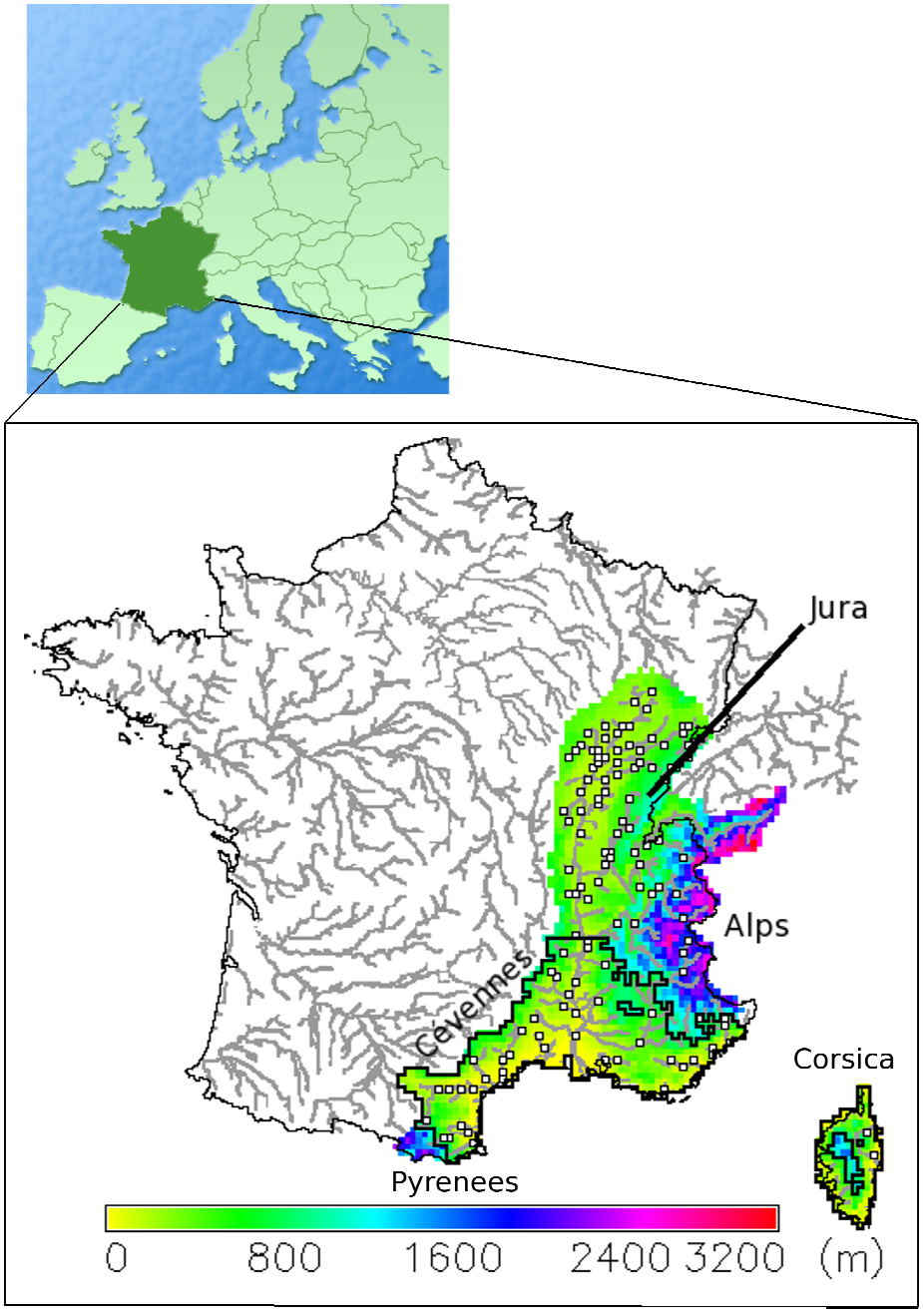

Fig. 1. Map of the domain studied (FullDom), indicating the elevation and the river network. The limit of the Mediterranean domain (MedDom) is indicated by the black line. The River gauges used in this study are indicated by the white dots.

and Planton, 1989; Noilhan and Mahfouf, 1996) and the hydrological model MODCOU (Modélisation couplée nappe-surface, Ledoux et al., 1989). Usually, ISBA-MODCOU is forced by the SAFRAN meteorological analysis (described below in Sect. 4.2). In our study, ISBA-MODCOU is forced by data derived from climate scenarios.

ISBA is a soil-vegetation-atmosphere transfer (SVAT) scheme. It is used to simulate the exchanges in heat, mass, momentum, and carbon (if relevant) between the continental surface (including vegetation and snow) and the atmosphere. In SIM (Habets et al., 2008), the three-layer force restore version of the model is used (Boone et al., 1999), together with the explicit multilayer snow model (Boone and Etchevers,

2001). It accounts for a subgrid runoff (Habets et al., 1999b) and a subgrid drainage schemes (Habets et al., 1999a). All these options were used in this study.

The formulation of stomatal conductance in the original version of ISBA (ISBA-Standard) represents the impact of the photosynthetically active radiation on stomatal aperture, the soil water stress, the vapor pressure deficit of the atmosphere, and the air temperature (Jarvis, 1976). In order to simulate the direct effect of CO_2 on plant physiology, a CO_2-responsive version of ISBA (ISBA-A-gs) has been developed. ISBA-A-gs (Calvet et al., 1998) simulates the stomatal conductance considering the functional relationship between the stomatal aperture and photosynthesis, based on the biochemical A-gs model proposed by Jacobs et al. (1996) under well watered conditions. The CO_2 concentration in the atmosphere is taken into account explicitly by the photosynthesis model. The model also includes a representation of the soil moisture stress using two plant responses to drought, depending on the vegetation type (Calvet, 2000, Calvet et al., 2004). ISBA-A-gs also simulates the green LAI, by using a simple vegetation growth model (Calvet and Soussana, 2001). The model simulates two aboveground biomass reservoirs: the leaf biomass and the aboveground structural biomass. The reservoirs are fed by the net assimilation of CO_2, and decreased by turnover and respiration terms. Phenology is modeled implicitly: the leaf biomass turnover term is driven by photosynthesis, and LAI is proportional to the leaf biomass. Nitrogen dilution limits the CO_2 fertilization effect, which tends to increase the biomass. In this study, nitrogen dilution is accounted for by parameterizing the change in leaf nitrogen mass-based concentration N_L in response to a rise in CO_2 concentration. This parameterization has been proposed by Calvet et al. (2008): the sensitivity of leaf nitrogen concentration versus CO_2 concentration is accounted for by using the meta-analysis of the literature carried out by Yin (2002). ISBA-A-gs has been tested and validated at local (e.g. Sabater et al., 2007) and global scales (Gibelin et al., 2006)

Within a grid box, ISBA can be run on each of the 12 land surface types (bare land, bare rock, permanent snow and ice, deciduous broadleaf forest, evergreen broadleaf forest, needle-leaved forest, C3 crops, C4 crops, irrigated crops, C3 herbaceous, C4 herbaceous, wetlands) represented by the model, or using aggregated parameters. In order to take the variability of ecosystems within a grid box into account, ISBA-A-gs can only be run in a tile version: in each grid box, the model simulates the evolution of the prognostic variables for each vegetation type (or patch) that is present in the grid box. Fluxes and LAI are averaged over the grid box. In this study, ISBA-Standard is used in the same tile configuration to facilitate the comparisons. In both cases, the parameters of the model are given by the ECOCLIMAP2 physiographic database, described in the next section. The tiled version of ISBA-Standard and ISBA-A-gs used in this study, as well as ECOCLIMAP2, are imbedded into SURFEX (SURFace Externalisée, Martin et al., 2007), the surface modeling platform of Météo-France. Table 1 summarizes the characteristics of the different versions of ISBA used in this study.

The surface runoff and bottom drainage calculated by ISBA over each grid box are transferred to the hydrogeological model MODCOU (Ledoux et al., 1989). MODCOU calculates the temporal and spatial evolution of the aquifer (if present) using the diffusivity equation. Then it calculates the interaction between the aquifer and the river and finally routes the surface water to the rivers and within the rivers using an isochronistic algorithm. It calculates river discharges with a time step of three hours. The time step used to calculate the evolution within the aquifer is 1 day. In this version of MODCOU, only the major aquifers are simulated. Hence, only Rhône/Saône aquifer is explicitly simulated in the region under study. The other aquifers are simulated using the subgrid drainage parametrization.

The resolution of ISBA is 8 km, while the resolution of MODCOU varies between 1 and 64 km, according to the terrain.

4 Databases

4.1 Soil and vegetation database

The vegetation parameters (albedo, emissivity, roughness length, LAI, vegetation fraction, and physiological parameters) are given by the ECOCLIMAP2 (Faroux et al., 2009) database, which is a recent update of the ECOCLIMAP database (Masson et al., 2003) over Europe. ECOCLIMAP2 provides a coherent ensemble of key parameters for ISBA at a wide range of horizontal scales. The general strategy for mapping the surface is achieved in two steps. First, a land cover classification is set up to gather pixel values that are consistent in terms of NDVI values derived from the AVHRR sensor. Second, on the basis of the classification and using existing land cover maps, lookup tables allow similar values of surface parameters to be assigned to all the pixels of the same class. The LAI estimate of ECOCLIMAP2 is based on the MODIS LAI product, collection 4 (Yang et al., 2006). The MODIS data are available at a spatial resolution of 1/120° and a temporal resolution of 8 days. They are linearly interpolated to fit the ECOCLIMAP2 10-day temporal resolution and its 1-km spatial resolution.

The soil texture information (clay and sand proportions) for all runs comes from the soil geographical database (BDGSF) of the French Institut National de Recherche Agronomique (http://www.gissol.fr/programme/bdgsf/bdgsf.php). This base uses the FAO methodology to determine soil types suited to the French context. France is divided into typical soil units with homogeneous properties, based on regional sampling.

Table 1. Summary of the different versions of ISBA used and their characteristics.

Name	Version of ISBA	Main characteristics	Number of patches	Database used	Simulations
STD12P	Standard	– evapotranspiration calculated with Jarvis formula	12	ECOCLIMAP2	Present climate End of 21st century
A-gs	A-gs	– sensitive to CO_2 concentration – water stress non-linear – simulation of LAI – Nitrogen dilution effect taken into account	12	ECOCLIMAP2	Present climate End of 21st century
A-gs/NoCO2N	A-gs	Same as A-gs except: – CO_2 concentration is kept at its 1970–2000 value (350 ppm) – Leaf Nitrogen is constant	12	ECOCLIMAP2	End of 21st century

4.2 Atmospheric database, climate scenario, and downscaling

We consider two 30-yr periods in this study: the first is August 1970 – July 2000 (present climate); and the second is August 2069 – July 2099 (end of the 21st century).

The reference atmospheric database for the present climate was provided by the SAFRAN (Système d'Analyse Fournissant des Renseignements à la Neige) meteorological analysis, as in Quintana-Seguí et al. (2010). SAFRAN (Durand et al., 1993) produces an analysis of near surface atmospheric variables at a resolution of 8 km using observations from the automatic, synoptic, and climatologic networks of Météo-France and a first guess from a large scale operational weather prediction model. For most atmospheric variables, the analysis is made using optimal interpolation, but for incoming solar radiation and downward infrared radiation, SAFRAN uses a radiative transfer scheme (Ritter and Geleyn, 1992). A more detailed description of SAFRAN can be found in Quintana-Seguí et al. (2008). The data were interpolated over the 8 km grid used to force ISBA. The accuracy of the SAFRAN atmospheric forcing has been evaluated by Quintana-Seguí et al. (2008) and Vidal et al. (2010).

Future climate data were derived from an IPCC SRES A2 simulation performed with the coupled Sea Atmosphere Mediterranean Model (Somot et al., 2008). This model results from the coupling of an atmospheric model with an oceanographic model. The atmospheric model is ARPEGE-Climate (Gibelin and Déqué, 2003), zoomed on the Mediterranean region at a resolution of 50 km; and the oceanographic model is OPAMED (Somot, 2005; Somot et al., 2006), with a resolution of about 10 km over the Mediterranean Sea. For the 21st century, the simulation was done using the IPCC SRES A2 (high economic and demographic growth, Nakicenovic et al. 2000) and covered a period of 140 yr: 1961–2099. This simulation was performed in the framework of the French CYPRIM project (http://www.cnrm.meteo.fr/cyprim/) and will be referred to as "CYPRIM" or "CYP" in the following.

This simulation was then downscaled to the 8 km grid using the classical quantile mapping method (Wood et al., 2004; Déqué et al., 2007) described by Quintana-Seguí et al. (2010). The variables needed to force ISBA (precipitation, temperature, wind speed, humidity, solar radiation and downward atmospheric radiation) simulated by the GCM according to their distribution came from the reference database (SAFRAN). For each cell, a correction was calculated for each percentile of the distribution of each variable of interest at the daily time step by comparing the observed distribution to that of the closest model cell. Each season was treated separately. To interpolate the variables into the hourly time step (from the daily time step), which was necessary for the hydrological model, a mean daily cycle was calculated for each variable using SAFRAN. For the temperature, the correction was calculated for the daily maximum and minimum; hence, the daily cycle was modified according to these two variables.

4.3 Discharge database

Discharges at a total of 204 stations (Fig. 1) were simulated by MODCOU over the area. Among them, a subset of 177 stations with sufficient data of good quality was selected to validate the model simulations for the present climate. The selected stations covered the whole of the studied domain, had very few missing data, and according to the "Banque hydro" (http://www.hydro.eaufrance.fr), were not seriously affected by anthropization (for example hydropower generation facilities or irrigation for agriculture). For the comparison with the future climate, all stations were used.

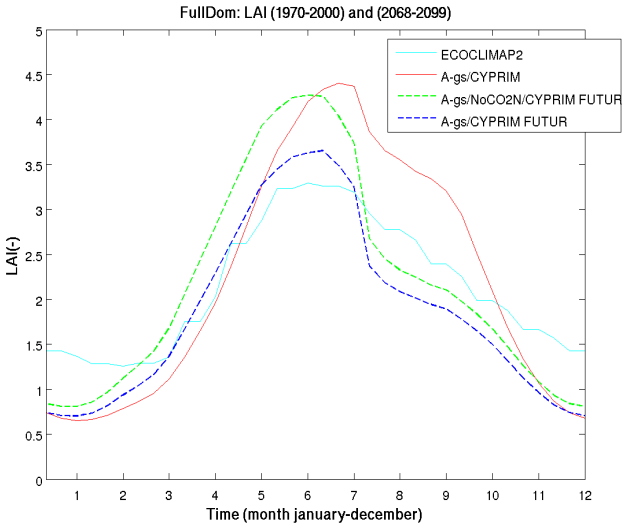

Fig. 2. Mean annual cycle of LAI for the full domain (FullDom), averaged over 1970–2000 for the ECOCLIMAP2 database, and for ISBA-A-gs with the CYPRIM forcing (A-gs/CYPRIM), and averaged over 2069–2099 for ISBA-A-gs with the CYPRIM scenario (A-gs/CYPRIM FUTUR), and for ISBA-A-gs/NoCO2N with the CYPRIM scenario (A-gs/NoCO2N/CYPRIM FUTUR).

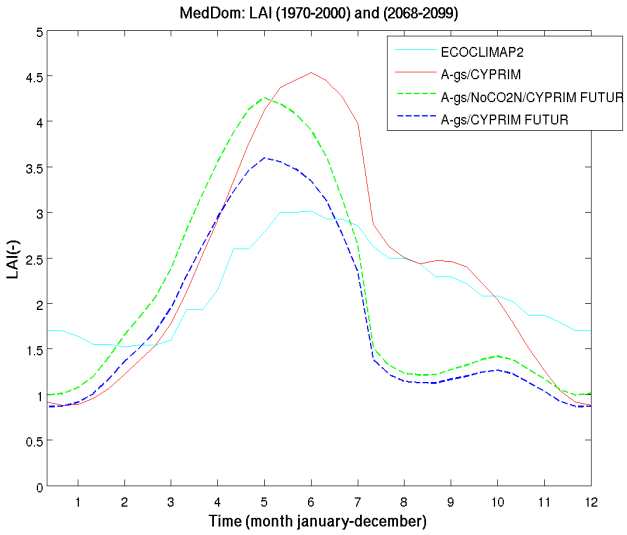

Fig. 3. Mean annual cycle of LAI for the Mediterranean Domain (MedDom), averaged over 1970–2000 for the ECOCLIMAP2 database and for ISBA-A-gs with CYPRIM climate scenario (A-gs/CYPRIM), and averaged over 2069–2099 for ISBA-A-gs with CYPRIM scenario (A-gs/CYPRIM FUTUR) and for ISBA-A-gs/NoCO2N with CYPRIM scenario (A-gs/NoCO2N/CYPRIM FUTUR).

5 Present climate simulations

The twelve-patch versions of ISBA-Standard and ISBA-A-gs were run with the downscaled CYPRIM forcing over the 1970–2000 period. A two-year spin up was performed in order to initialize ISBA, while the initial state of MODCOU was taken from the existing long-term simulation of Quintana-Seguí et al. (2010).

5.1 Meteorological variables

Table 2 compares the yearly and seasonal CYPRIM temperature and precipitation data with the reference SAFRAN analysis for the FullDom and MedDom domains.

For FullDom, the CYPRIM scenario underestimates the reference SAFRAN mean annual air temperature by 0.33 °C. The underestimation reaches 0.64 °C in winter. This bias was noted by Quintana-Seguí et al. (2010) who explained the difference by the fact that the downscaling method was calibrated on a different period than the period studied here. Regarding precipitation, the annual averages are very close – even at the seasonal scale. When considering the southern part of the domain (MedDom) only, the same type of difference between SAFRAN and CYPRIM is observed. It should be noted that precipitation is lower and air temperature higher than for FullDom.

5.2 LAI

Figure 2 shows the FullDom mean annual cycle of LAI simulated by ISBA-A-gs together with the ECOCLIMAP2 estimates. The LAI estimated by ECOCLIMAP2 presents an annual cycle with a minimum value ($1.2\,m^2\,m^{-2}$) in February and a maximum ($3.3\,m^2\,m^{-2}$) at the end of June. After this peak, the LAI decreases steadily until winter. The annual cycle of the LAI simulated by ISBA-A-gs is more pronounced and presents different behavior. The minimum LAI is reached in January and is lower ($0.6\,m^2\,m^{-2}$), and the maximum LAI is reached in July ($4.3\,m^2\,m^{-2}$). The ISBA-A-gs LAI is lower than the ECOCLIMAP2 reference in wintertime and springtime, and higher than ECOCLIMAP2 during the other seasons. For the Mediterranean part of the domain (Fig. 3), the ECOCLIMAP2 LAI cycle is less pronounced than for the whole domain (1.5 to $3.0\,m^2\,m^{-2}$); and this tendency, although attenuated, is also reproduced by ISBA-A-gs.

This general behavior masks significant local variations. The spring LAI (Fig. 4) presents significant differences between ISBA-A-gs and ECOCLIMAP2. A good agreement can be seen for the Alpine vegetation and in Corsica. In the northern part of the domain, ISBA-A-gs underestimates the LAI, both in plain areas and in mid elevation mountains (Jura). In these regions, there is a delay of about one month in the vegetation onset. These results are consistent with the result of Brut et al. (2009) that pointed out, despite

Table 2. Average precipitation (mm d^{-1}), air temperature (°C), total runoff (mm d^{-1}) and, evapotranspiration (mm d^{-1}) on the full domain (FullDom) and for the southern part of the domain (MedDom) for the end of the 20th century. SAF corresponds to the SAFRAN gridded database, CYP to the CYPRIM climate forcing, A-gs/CYP to the ISBA-A-gs version with the CYPRIM scenario, and STD12P/CYP to the ISBA-Std12P version with the CYPRIM scenario.

1970–2000	Precipitation		Temperature		Total Runoff		Evapotranspiration	
				FullDom				
	SAF	CYP	SAF	CYP	A-gs/CYP	STD12P/CYP	A-gs/CYP	STD12P/CYP
Year	3.02	3.02	9.52	9.19	1.70	1.57	1.32	1.44
DJF	3.17	3.12	2.50	1.86	1.92	1.87	0.34	0.43
MAM	2.92	2.94	8.26	7.96	2.17	1.95	1.50	1.80
JJA	2.44	2.42	17.34	17.21	1.31	1.17	2.46	2.51
SON	3.55	3.60	9.99	9.71	1.40	1.29	0.96	1.04
				MedDom				
	SAF	CYP	SAF	CYP	A-gs/CYP	STD12P/CYP	A-gs/CYP	STD12P/CYP
Year	2.42	2.43	12.58	12.24	1.08	0.99	1.35	1.43
DJF	2.67	2.71	5.70	5.08	1.94	1.85	0.55	0.69
MAM	2.43	2.43	11.11	10.79	1.12	0.95	1.90	2.14
JJA	1.43	1.39	20.42	20.30	0.24	0.21	2.03	1.90
SON	3.16	3.19	13.09	12.80	1.01	0.97	0.91	1.03

the large uncertainty in satellite LAI retrievals, the difficulties of ISBA-A-gs in simulating the leaf onset of C3 crops and of mountainous grasslands over southwestern France. Lafont et al. (2010) confirmed such a delay, with regional variations in a study at the scale of France. In contrast, the ISBA-A-gs LAI is higher in most of the low lying area in the south of the domain, an area close to the MedDom domain. Another difference with the satellite estimates is the strong LAI decrease in this region in July (Fig. 3), in relation with the limitation of the water available for plant growth, followed by a weak secondary maximum in September after the first autumn rainfalls.

5.3 Water balance

The average evapotranspiration and total runoff are shown in Table 2. On a yearly basis, the ISBA-A-gs evapotranspiration (1.32 mm d^{-1}) is lower than the evapotranspiration simulated by ISBA-Standard (1.44 mm d^{-1}). This difference is maximum during spring and can be attributed to differences in the formulation of evapotranspiration in the models as the LAI of both models are of the same order of magnitude, as shown in Fig. 2 (the prescribed LAI for ISBA-Standard is derived from ECOCLIMAP2). The differences are less marked in the other seasons, especially in autumn and winter when evapotranspiration is low. In summer, the evapotranspiration is maximum in both models.

The MedDom domain is characterized by lower precipitation, higher air temperature, and a significantly lower snow cover than the full domain. In consequence, the annual evapotranspiration rate is of the same order of magnitude as for the full domain, but the seasonal distribution is modified. Evapotranspiration is higher in winter and spring than in FullDom because of the absence of a significant snow cover. It is lower in summer because of drier soils in this part of the domain. In autumn, on average, the rain reaches a maximum and the evapotranspiration is almost equivalent to the value for the entire domain.

The total runoff simulated by ISBA-A-gs is higher than for the ISBA-Standard (1.70 mm d^{-1} for ISBA-A-gs versus 1.57 mm d^{-1} for ISBA-Standard, yearly).

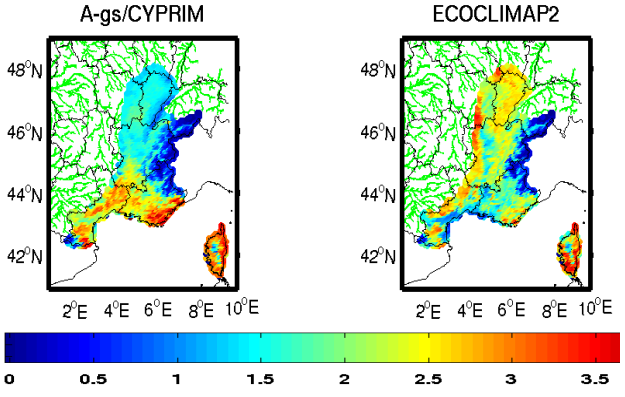

Fig. 4. Springtime LAI averaged over 1970–2000 for the A-gs version of ISBA with CYPRIM climate forcing (A-gs/CYPRIM), and for the ECOCLIMAP2 database.

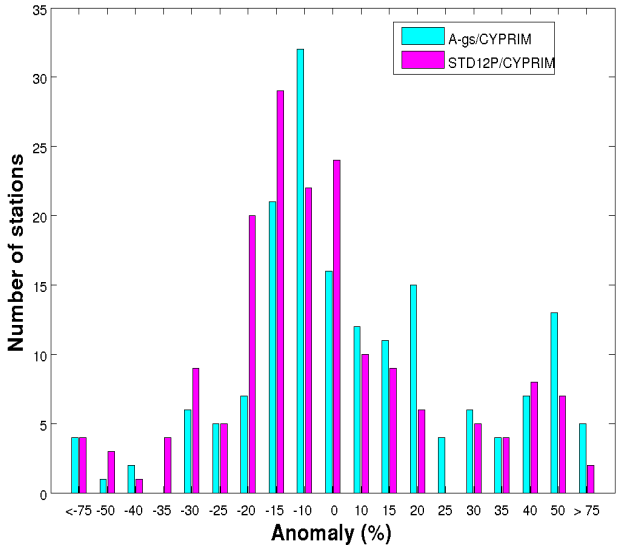

Fig. 5. Histogram of the number of stations in each class of anomaly of discharge for ISBA-A-gs and ISBA-Standard with the CYPRIM climate forcing when compared to observations. Data are for the annual mean.

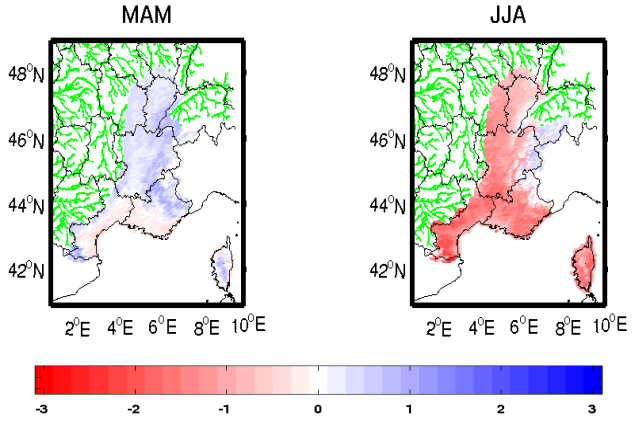

Fig. 6. Anomalies of average seasonal LAI (March-April-May and June-July-August) obtained with ISBA-A-gs. The anomalies are calculated by comparing two periods: 2069–2099 vs. 1970–2000.

For the MedDom, the runoff is considerably lower (63 % of the value of the full domain on a yearly basis). The difference is more pronounced in spring in relation to the snowmelt. While the total runoff represents 43 % of the total precipitation in MedDom, this proportion reaches 55 % for FullDom (ISBA-A-gs).

5.4 Discharge

The discharges simulated by the model were compared to the discharges observed at the stations described in Sect. 4.3 and shown in Fig. 1. The ISBA-Standard anomaly is +1.8 %, so the standard model performs better than ISBA-A-gs (+10.0 %) here. This result is consistent with the differences shown in Table 2 (higher runoff and lower evapotranspiration for ISBA-A-gs). Figure 5 shows the dispersion of the scores for individual stations. The distribution of error is similar for both models but ISBA-A-gs presents a general shift toward higher anomalies.

6 Future climate simulations

The impact of climate change was investigated using the ISBA-A-gs and the ISBA-Standard versions in order to assess the impact of the direct effect of CO_2 on vegetation and on hydrology. In addition, a third run was executed with a specific version of ISBA-A-gs in which the CO_2 concentration was left at its present value and the nitrogen dilution was simulated with the present CO_2 value (ISBA-A-gs/NoCO2N). The objective of this run was to evaluate the effect on the vegetation behavior and hydrological variables when changes were applied to the meteorological forcing only. Three 30-yr simulations (August 2069–July 2099) were performed with the downscaled CYPRIM data in a manner similar to the present climate runs.

6.1 Meteorological variables

The air temperature and precipitation anomalies of the climate scenario are shown in Table 3. The climate scenario results in a significant annual precipitation decrease for FullDom (−10 %). The most affected season is summer (−20 %), while winter precipitation remains stable. The same trend is found for MedDom (−13 % for the annual average): the spring and summer seasons present the largest decreases (–20 and –30 %, respectively). Yearly air temperature anomalies are +3.5 °C for both domains. The maximum air temperature anomaly is found in summer, while the minimum anomaly is found in spring for FullDom and MedDom.

6.2 Snow processes

The impact of snow processes is identical in all models as they share the same snow model. The simulated snow cover diminishes drastically at all elevations. In winter the impact is marked at low and mid elevation and the snow-free area is significantly increased. In consequence, the evapotranspiration increases in all models (+30 to +33 % for FullDom, Table 3). On other areas, the increase is only due to the warmer conditions and is therefore smaller (+15 to +18 % for MedDom). The discharge increases significantly in mountainous regions because the proportion of rainfall and the snowmelt increase in winter. The impact on snow cover can also be seen in spring, a season were the evapotranspiration increases in mountainous areas (+7.3 % to +17 % for FullDom).

Table 3. Same as Table 2 but for the end of the 21st century and the corresponding anomalies with 1970–2000. A-gs/NoCO2N/CYP corresponds to the ISBA-A-gs version with the CYPRIM scenario and no CO_2 effect.

2069–2099	Precipitation		Temperature		Total Runoff			Evapotranspiration		
					FullDom					
	CYP		CYP		A-gs/CYP	A-gs/NoCO2N/CYP	STD12P/CYP	A-gs/CYP	A-gs/NoCO2N/CYP	STD12P/CYP
Year	2.72	(−10 %)	12.73	(+3.5)	1.4 (−18 %)	1.38 (−19 %)	1.31 (−17 %)	1.32 (+0.3 %)	1.34 (+1.6 %)	1.41 (−2.6 %)
DJF	3.16	(+1.1 %)	5.41	(+3.5)	2.09 (+8.9 %)	2.08 (+8 %)	2.02 (+8 %)	0.45 (+30 %)	0.46 (+33 %)	0.56 (+31 %)
MAM	2.62	(−11 %)	10.69	(+2.7)	1.7 (−21 %)	1.68 (−22 %)	1.56 (−20 %)	1.7 (+13 %)	1.75 (+17 %)	1.93 (+7.3 %)
JJA	1.93	(−20 %)	21.72	(+4.5)	0.75 (−43 %)	0.74 (−43 %)	0.68 (−42 %)	2.3 (−6.5 %)	2.31 (−6.1 %)	2.2 (−12 %)
SON	3.16	(−12 %)	13.08	(+3.3)	1.04 (−26 %)	1.02 (−27 %)	0.99 (−24 %)	0.83 (−13 %)	0.83 (−13 %)	0.93 (−10 %)
					MedDom					
	CYP		CYP		A−gs /CYP	A−gs/NoCO2N /CYP	STD12P /CYP	A−gs /CYP	A−gs/NoCO2N /CYP	STD12P /CYP
Year	2.11	(−13 %)	15.75	(+3,5)	0.87 (−19 %)	0.86 (−20 %)	0.82 (−18 %)	1.24 (−8.1 %)	1.25 (−7.1 %)	1.29 (−9.7 %)
DJF	2.74	(+1.3 %)	8.33	(+3.2)	1.73 (−11 %)	1.71 (−12 %)	1.64 (−11 %)	0.64 (+16 %)	0.65 (+18 %)	0.8 (+15 %)
MAM	1.95	(−20 %)	13.51	(+2.7)	0.86 (−24 %)	0.83 (−25 %)	0.75 (−21 %)	1.94 (+0.6 %)	1.95 (+3 %)	2.04 (−3.5 %)
JJA	0.98	(−30 %)	25.0	(+4.7)	0.16 (−33 %)	0.16 (−34 %)	0.15 (−29 %)	1.64 (−19 %)	1.63 (−19 %)	1.44 (−24 %)
SON	2.75	(−14 %)	16.14	(+3.3)	0.74 (−27 %)	0.73 (−28 %)	0.72 (−25 %)	0.76 (−16 %)	0.76 (−16 %)	0.9 (−12 %)

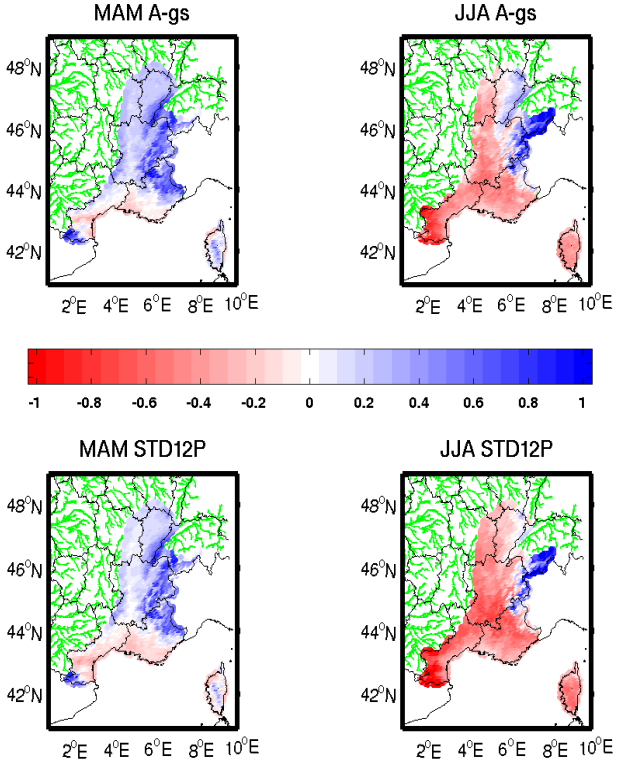

Fig. 7. Anomalies of average seasonal evapotranspiration (March-April-May and June-July-August) obtained with ISBA-A-gs (top) and ISBA-Standard (bottom) with the CYPRIM scenario for both. The differences are calculated by comparing two periods: 2069–2099 vs. 1970–2000.

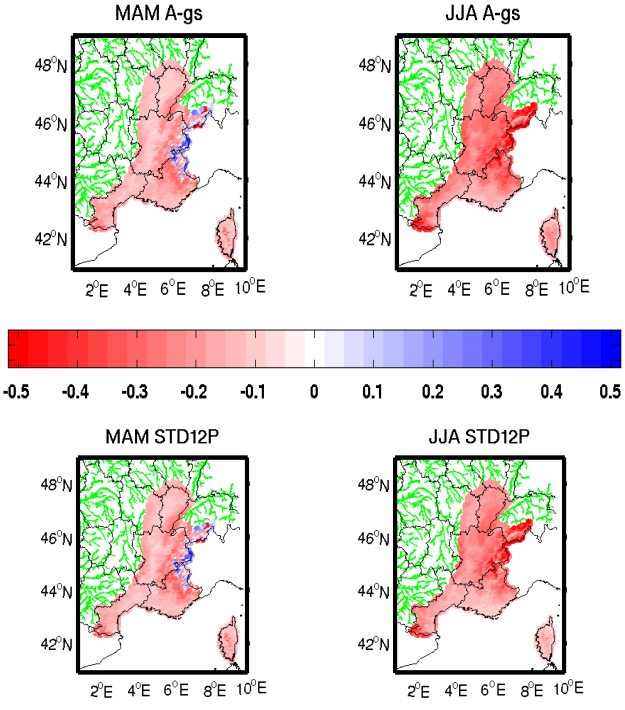

Fig. 8. Anomalies of average seasonal SWI (March-April-May and June-July-August) obtained with ISBA-A-gs (top) and ISBA-Standard (bottom) with the CYPRIM scenario for both. The anomalies are calculated by comparing two periods: 2069–2099 vs. 1970–2000.

6.3 Impact on vegetation

While ISBA-Standard assumes an unchanged seasonal LAI distribution, ISBA-A-gs calculates the LAI dynamically, assuming that no change in land cover or land use occurs. The mean LAI time series corresponding to the end of the 21st century is shown in Figs. 2 and 3 for the two domains (dashed curve). Over FullDom, the ISBA-A-gs LAI (blue dashed curve) occurs slightly earlier and the maximum is lower than

for the present climate ($3.6\,m^2\,m^{-2}$). The inclusion of the vegetation response to the direct effect of the CO_2 concentration and the nitrogen dilution tends to diminish the LAI but has almost no effect on the date of the maximum. Then there is a rapid decrease in July, more pronounced than in the present climate. The impact on LAI is maximum from June to October. When looking at aggregated results for MedDom in the future climate (Fig. 3), the most striking feature is that the LAI during the August-October period is very close to its winter value, indicating profound changes in the vegetation cycle. The secondary maximum persists, but occurs at the end of October.

Figure 6 shows the anomalies of springtime and summertime LAI of ISBA-A-gs between 2069–2099 and 1970–2000. In spring, the LAI decreases in most low lying areas. In summer, the LAI anomaly is negative over most parts of the domain except in mountain areas. The diminution seems smaller near the Mediterranean shore west of the Rhone, but this is only due to high proportion of bare soil (40 %) in this region (both models share the same bare soil evaporation parameterization). In high mountains, there is a large increase in the LAI of grassland as a consequence of reduced snow, warmer seasonal conditions, and water availability. The impact is neutral at mid elevations in the Alps and in the Jura mountains where conifer forests and grassland coexist.

In the ISBA-A-gs/NoCO2N run, the leaf onset occurs earlier (by about one month) in Figs. 2 and 3. Over FullDom, the annual maximum LAI is reached earlier and is almost the same as for the present climate ($4.3\,m^2\,m^{-2}$ versus $4.4\,m^2\,m^{-2}$ in the present climate). The spatial variations follow the same patterns as the ISBA-A-gs run. The differences in the two versions are especially marked at the onset of vegetation and during spring. On average, the fertilization and antitranspirant effect, combined with the nitrogen dilution, tends to limit the simulated LAI when compared to the ISBA-A-gs/NoCO2N run. The latter run illustrates that the vegetation response to an exceptionally hot year under the present climate does not correctly predict the vegetation behavior under future conditions.

6.4 Evapotranspiration and soil wetness

Evapotranspiration anomalies (Fig. 7 for ISBA-A-gs and ISBA-Standard) are highly variable over the domain. In spring, there is a decrease in the south of the domain, especially along the Mediterranean coast, while evapotranspiration increases in other parts of the domain. The maximum increase is located in the mountain area, in relation with the reduced snow coverage and vegetation development for the ISBA-A-gs version. ISBA-A-gs shows a tendency toward more evapotranspiration when compared to ISBA-Standard, with a difference that is quite evenly distributed: increased evapotranspiration in the mountain area, smaller decrease in the other regions. Both versions give very similar values in the coastal zone where the bare soil proportion reaches 40 %. Averaged over the whole domain, ISBA-Standard has the lowest increase in evapotranspiration (+7.3 % for FullDom, Table 3), the two versions of ISBA-A-gs present a higher increase in evapotranspiration (+17 % for ISBA-A-gs/NoCO2N, +13 % for ISBA-A-gs, Table 3).

In summer, the ISBA-Standard variation is more pronounced than for ISBA-A-gs versions (−12 % for ISBA-Standard versus −6 % for ISBA-A-gs and ISBA-A-gs/NoCO2N, Table 3). It should be noted that, at the same time, the SWI variations are more pronounced in the ISBA-A-gs version than in the ISBA-Standard version (Fig. 8).

In autumn, in relation with the drastic diminution of the LAI in ISBA-A-gs, this model presents a more pronounced decrease of evapotranspiration than ISBA-Standard.

The soil wetness variations are consistent with the changes already discussed for the LAI and evapotranspiration. Figure 8 shows anomalies of SWI for ISBA-A-gs and ISBA-Standard between future and present climates in spring and in summer. In spring, both versions simulate a soil wetness lower than in the present climate, except in mountain areas (advanced snowmelt) for spring. The decrease in terms of spatial distribution and intensity is very similar in both versions. In summer, the soil moisture decrease is more pronounced, with a maximum in the mountains (Alps and Pyrenees). However, in very high mountains, the soil remains well watered and allows enhanced vegetation development (Fig. 6). Generally, ISBA-A-gs and ISBA-Standard present the same spatial and temporal behavior. However, in summer, ISBA-A-gs variation is higher over the entire domain as a consequence of a different annual cycle for both evapotranspiration and vegetation.

6.5 Discharge

Figure 9 shows the spatial distribution of the anomalies of the mean seasonal discharge associated with their significance for ISBA-A-gs. The significance of the anomalies was evaluated using an adaptation of the Student's test that does not require the assumption of equality of the variances of the compared samples. This adaptation is often referred to as Welch's test (Welch, 1947).

The highest increases in winter discharges are located in the mountainous part of the domain (Alps, Jura, eastern Pyrenees), while in most areas, a slight decrease is observed. In spring the decrease is more pronounced near medium elevation mountains (Jura and eastern Pyrenees), while an increase is observed in a few gauging stations of the central Alps only. The decrease is maximum over the whole domain in summer. In autumn, due to increased precipitation, the impact is less pronounced in the south (with some gauges recording increased discharges). However, the changes are significant in the north of the domain (Saône plain and the foothills of Jura). The presence of an aquifer that smoothes the hydrological response to climate explains the specific response of this region.

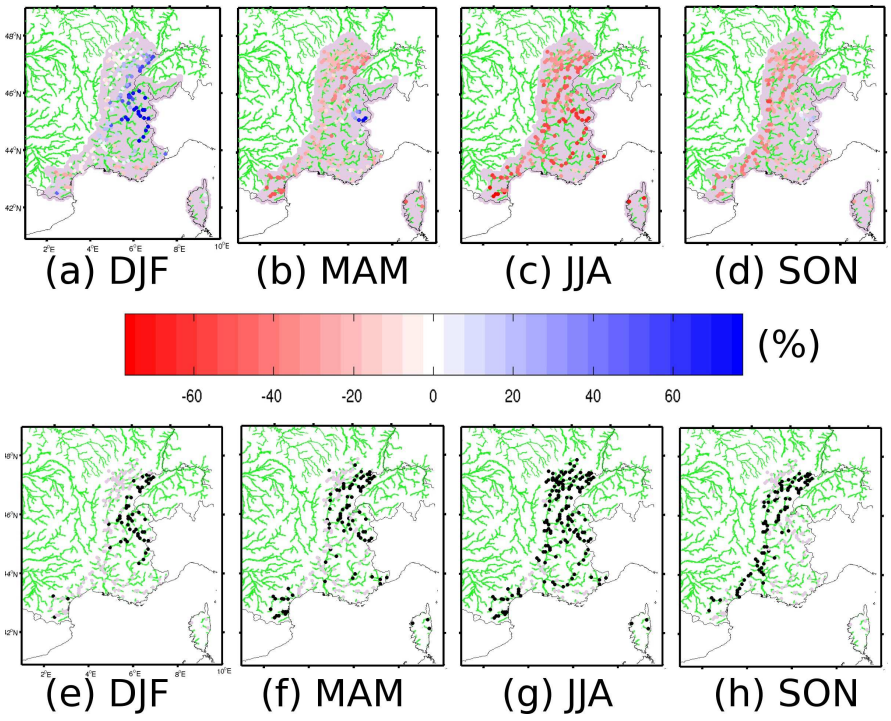

Fig. 9. First row: anomalies of average seasonal discharge obtained with ISBA-A-gs. Second row: significance of the anomalies: black means that the changes are statistically significant and light grey means they are not. The anomalies are calculated by comparing two periods: 2069–2099 vs. 1970–2000.

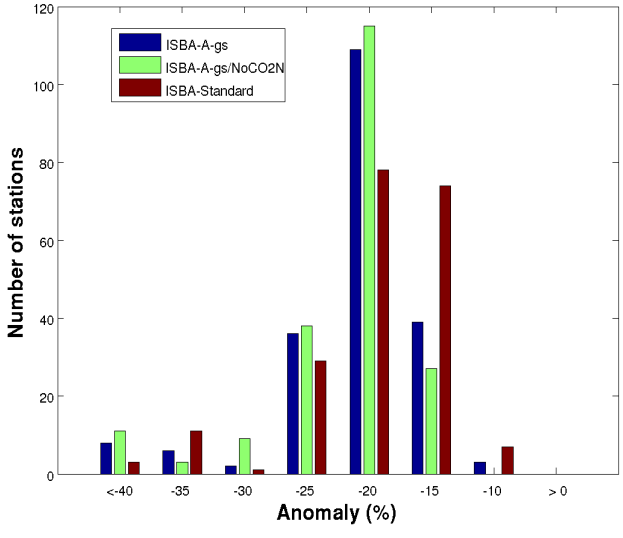

Fig. 10. Histogram of the number of stations in each class of annual anomaly of discharge between the future climate and the present climate according to ISBA-A-gs, ISBA-A-gs/NoCO2N, and ISBA-Standard.

Figure 10 shows the statistical distribution of the anomalies of impact of the climate scenario on all the gauges,

Table 4. Number of stations with significant changes at the end of the 21st century (compared to 1970–2000) for the different model versions at the yearly and seasonal time scales (out of 204 stations).

	YEAR	DJF	MAM	JJA	SON
STD12P	116	52	93	170	84
A-gs	131	61	106	173	100
A-gs/NoCO2N	139	61	113	181	108

confirming that the impact is more pronounced with ISBA-A-gs. On average, the anomaly is −24 % with ISBA-A-gs/NoCO2N, −23 % with ISBA-A-gs, and −22 % with ISBA-Standard, which is consistent with the anomalies of the total runoff (−19 %, −18, and −17 %, respectively).

Table 4 presents the number of stations where the changes are significant for each model and for each season and on an annual basis. In all seasons, ISBA-Standard presents the smallest number of stations with significant changes. The most important differences between ISBA-Standard and ISBA-A-gs models are seen for the year and for autumn (a season with marked hydrological changes in ISBA-A-gs). These results show that the explicit treatment of the vegetation response to climate change tends to increase the

hydrological impact of climate change. With a greater effect on LAI and evapotranspiration, ISBA-A-gs/NoCO2N shows the highest impact.

7 Conclusions

This study is a contribution to the question of uncertainty caused by the impact model in climate change studies. Specifically, we studied how the inclusion of a dynamic vegetation scheme in the ISBA land surface model affected the hydrological impact on the continental surface in the context of an increased atmospheric CO_2 concentration. The study focused on the Mediterranean area of France. The impact on hydrological variables simulated by ISBA-Standard (with prescribed vegetation), and ISBA-A-gs (with dynamical vegetation), were compared using the same downscaled SRES A2 climate scenario.

In present climate conditions, ISBA-Standard obtained better results than ISBA-A-gs, which slightly overestimated the observed discharges over the area. In addition, ISBA-A-gs presented a different LAI distribution, with higher LAI than ECOCLIMAP2 in summer and autumn.

At the end of the 21st century, on a yearly basis, both ISBA-A-gs and ISBA-Standard agreed on a decrease of total runoff (-18 % for ISBA-A-gs, -17 % for ISBA-Standard), but with seasonal and regional contrasts due to differences in the model physics. In winter, the general increase in evapotranspiration was similar in both models and could be attributed to the decrease in snow cover. The model differences could be seen clearly in spring and summer, with a tendency of ISBA-A-gs to evaporate more than ISBA-Standard (higher increase in mountainous regions, where evapotranspiration increases in both models, and smaller decrease in other regions). This difference illustrated the importance of the role of the vegetation changes in the response on a seasonal scale. The response of ISBA-A-gs was governed by the complex interaction of the CO_2 fertilization and antitranspirant effect, combined with the nitrogen dilution and increased soil stress. In contrast, the ISBA-Standard response was constrained by the unchanged LAI and stomatal conductance. This experiment showed that more significant changes in the hydrological impact were obtained using the version of ISBA that explicitly accounts for changes in the vegetation cycle.

An intermediate version of the ISBA-A-gs, with no changes in CO_2 concentration or nitrogen dilution, was used to evaluate the impact of changes only in the meteorological forcing. On average, the ISBA-A-gs/NoCO2N version presented higher variations in LAI and evapotranspiration than ISBA-A-gs, showing that the impact of the direct CO_2 effect on plant physiology combined with nitrogen dilution moderates the reaction of the model to changes in the meteorological forcing. The direct CO_2 effect and the nitrogen dilution in the model tended to reduce the impact on LAI and on spring and summer evapotranspiration, meaning that the nitrogen dilution is a key limiting factor for plant development in this region. However, given the large uncertainty in the leaf nitrogen response to an increase in CO_2 concentration and the fact that the formula proposed by Yin (2002) captured only 41 % of the variance of the sample, this result needs to be confirmed by studies with other land surface models. Another conclusion of this study is that the hydrological response in the future cannot be deduced from the hydrological response to anomalous years in the present climate.

The differences in total runoff impact, only 1 % between the two models, were lower than the differences found by Quintana-Seguí et al. (2010) for the same area by comparing three downscaling methods on the same scenario for the middle of the 21st century (7 %), and lower than the uncertainty associated with the GCM. It appeared that, at the scale of the region studied, ISBA-A-gs did not significantly modify previous conclusions obtained with ISBA-Standard on the hydrological budget. These quite small changes between the two versions of ISBA can be attributed to internal compensation effects, despite different evapotranspiration, water stress, and LAI variations formulations. Nevertheless, the use of a CO_2-responsive land surface scheme in climate impact assessment studies led to differentiated results, depending on the vegetation type (development of mountain vegetation and decrease of vegetation in the low lying areas) and on different seasonal responses. Only this version could modify the mean vegetation cycle, which is greatly affected in this region.

This study was a first attempt to use a CO_2-responsive version of ISBA for climate change impact studies at the regional scale, introducing some regional differences in the vegetation and water cycle when compared to the ISBA-Standard version. The modeling approach applied here provides a useful tool for assessing the effects of future climate changes. In addition, the ISBA-A-gs model allows more detailed studies on specific natural or managed vegetation types, as well as for agriculture, which is an important issue for future impact and adaptation studies. A further step would be to prescribe changes in the land cover and land use consistent with the climate change and according to the socioeconomic scenario. This possibility will be explored in future studies.

Acknowledgements. This work was supported by the VMC-2007 program of the French Agence Nationale de la Recherche (ANR) under the MEDUP project and by the ACI-FNS program “Aléas et Changements Globaux” of the French research ministry under the project CYPRIM. Discharge observations were provided by the French Hydro database (Ministère de l’Ecologie et du Développement Durable, Direction de l’Eau, http://www.eaufrance.fr), which gathers data from many producers. Sébastien Lafont was supported by the GEOLAND2 project, cofunded by the European Commission within the GMES initiative in FP7. The authors thank Samuel Somot and Aurélien Ribes for their support and the climate scenario used in this study.

Edited by: P. Drobinski
Reviewed by: B. van den Hurk and another anonymous referee

The publication of this article is financed by CNRS-INSU.

References

Boé, J., Terray L., Martin, E., and Habets, F.: Projected changes in components of the hydrological cycle in French river basins during the 21st century, Water Resour. Res., 45, W08426, doi:10.1029/2008WR007437, 2009.

Boone, A., Calvet, J. C., and Noilhan, J.: Inclusion of a third soil layer in a land surface scheme using the force-restore method, J. Appl. Meteorol., 38, 1611–1630, 1999

Boone, A. and Etchevers, P.: An inter-comparison of three snow schemes of varying complexity coupled to the same land-surface model: Local scale evaluation at an Alpine site, J. Hydrometeorol., 2, 374–394, 2001.

Brut, A., Rüdiger, C., Lafont, S., Roujean, J.-L., Calvet, J.-C., Jarlan, L., Gibelin, A.-L., Albergel, C., Le Moigne, P., Soussana, J.-F., Klumpp, K., Guyon, D., Wigneron, J.-P., and Ceschia, E.: Modelling LAI at a regional scale with ISBA-A-gs: comparison with satellite-derived LAI over southwestern France, Biogeosciences, 6, 1389–1404, doi:10.5194/bg-6-1389-2009, 2009.

Calvet, J.-C., Noilhan, J., Roujean, J.-L., Bessemoulin, P., Cabelguenne, M., Olioso, A., and Wigneron, J.-P.: An interactive vegetation SVAT model tested against data from six contrasting sites, Agric. For. Meteor., 92, 73–95, 1998

Calvet, J.-C.: Investigating soil and atmospheric plant water stress using physiological and micrometeorological data sets, Agric. For. Meteor., 103, 229–247, 2000.

Calvet, J.-C. and Soussana, J.-F.: Modelling CO2-enrichment effects using an interactive vegetation SVAT scheme, Agric. For. Meteor., 108, 129–152, 2001.

Calvet, J.-C., Rivalland, V., Picon-Cochard C., and Guehl, J.-M.: Modelling forest transpiration and CO2 fluxes – response to soil moisture stress, Agric. For. Meteorol., 124, 143–156, doi:10.1016/j.agrformet.2004.01.007, 2004.

Calvet, J.-C., Gibelin, A.-L., Roujean, J.-L., Martin, E., Le Moigne, P., Douville, H., and Noilhan, J.: Past and future scenarios of the effect of carbon dioxide on plant growth and transpiration for three vegetation types of southwestern France, Atmos. Chem. Phys., 8, 397–406, doi:10.5194/acp-8-397-2008, 2008.

Déqué, M., Rowell, D. P., Lüthi, D., Giorgi, F., Christensen, J. H., Rockel, B., Jacob, D., Kjellström, E., de Castro, M., and van den Hurk, B.: An intercomparison of regional climate simulations for Europe: assessing uncertainties in model projections, Climatic Change, 81 (May), 53–70, 2007.

Ducharne, A., Habets, F., Pagé, C., Sauquet, E., Viennot, P., Déqué, M., Gascoin, S., Hachour, A., Martin, E., Oudin, L., Terray, L., and Thiéry, D.: Climate change impacts on Water Resources and Hydrological Extremes in Northern France, XVIII Conference on Comp. Met. Water Res., June 2010, Barcelona, Spain, 2010.

Durand, Y., Brun, E., Merindol, L., Guyomarc'h, G., Lesaffre, B., and Martin, E.: A meteorological estimation of relevant parameters for snow models, Ann. Glaciol., 18, 65–71, 1993.

Faroux, S., Roujean, J.-L., Kaptué, A., and Masson, V. : La base de données ECOCLIMAP-II sur l'Europe, Note du Groupe de Météorologie à moyenne échelle, 86, 120, 1990.

Friedlingstein, P., Cox, P., Betts, R., Bopp, L., von Bloh, W., Brovkin, V., Cadule, P., Doney, S., Eby, M., Fung, I., Bala, G., John, J., Jones, C., Joos, F., Kato, T., Kawamiya, M., Knorr, W., Lindsay, K., Matthews, H. D., Raddatz, T., Rayner, P., Reick, C., Roeckner, E., Schnitzler, K.-G., Schnur, R., Strassmann, K., Weaver, A. J., Yoshikawa, C., and Zeng, N.: Climate and Carbon Cycle Feedback Analysis: Results from the C4MIP Model Intercomparison, J. Climate, 19, 3337–3353, 2006.

Gedney, N., Cox, P. M., Betts, R. A., Boucher, O., Huntingford, C., and Stott, P. A.: Detection of a direct carbon dioxide effect in continental river runoff records, Nature, 439, 835–838, doi:10.1038/nature04504, 2006.

Gibelin, A.-L., Calvet, J.-C., Roujean., J.-L., Jarlan, L., and Los, S .O.: Ability of the land surface model ISBA-A-gs to simulate leaf area index at the global scale: Comparison with satellites products, J. Geophys. Res., 111, D18102, doi:10.1029/2005JD006691, 2006.

Gibelin A. and Déqué, M.: Anthropogenic climate change over the Mediterranean region simulated by a global variable resolution model, Clim. Dyn., 20, 327–339, 2003.

Giorgi, F.: Climate change hot-spots, Geophys. Res. Let., 33, L08707, doi:10.1029/2006GL025734, 2006.

Giorgi, F. and Lionello, P.: Climate change projections for the Mediterranean region, Glob. Planet. Change, 63, 90–104, 2008.

Habets, F., Etchevers, P., Golaz, C., Leblois, E., Ledoux, E., Martin, E., Noilhan, J., and Ottle, C.: Simulation of the water budget and the river flows of the Rhone basin, J. Geophys. Res., 104, 31145–31172, 1999a.

Habets, F., Noilhan, J., Golaz, C., Goutorbe, J. P., Lacarrere, P., Leblois, E., Ledoux, E., Martin, E., Ottle, C., and Vidal-Madjar, D.: The Isba surface scheme in a macroscale hydrological model applied to the Hapex-Mobilhy area. part I: Model and database, J. Hydrol., 217, 75–96, 1999b.

Habets, F., Boone, A., Champeaux, J. L., Etchevers, P., Franchistéguy, L., Leblois, E., Ledoux, E., Le Moigne, P., Martin, E., Morel, S., Noilhan, J., and Quintana Seguí, P., Rousset-Regimbeau, F., and Viennot P.: The SAFRAN-ISBA-MODCOU hydrometeorological model applied over France, J. Geophys. Res., 113, D06113, doi:10.1029/2007JD008548, 2008.

Jacobs, C. M. J., van den Hurk, B. J. J. M., and de Bruin, H. A. R.: Stomatal behaviour and photosynthetic rate of unstressed grapevines in semi-arid conditions, Agric. For. Meteorol., 80, 111–134, 1996.

Jarvis, P. G.: The interpretation of the variations in leaf water potential and stomatal conductance found in canopies in the field, Phil. Trans. Roy. Soc. London, B273, 593–610, 1976.

Lafont, S., Zhao, Y., Barbu, A., Carrer, D., Calvet, J.-C., Peylin, P., and Weiss, M.: High resolution simulation of LAI, carbon and water fluxes over France. Earth Observation for Land-Atmosphere Interaction Science, Proceedings ESA-iLEAPS-EGU joint Conference 2010, ESA Special Publications SP-688,

2010.

Leander, R., Buishand, T. A., van den Hurk, B. J., and de Wit, M. J.: Estimated changes in flood quantiles of the river Meuse from resampling of regional climate model output, J. Hydrol., 351, 331–343, 2008.

Ledoux, E., Girard, G., De Marsily, G., and Deschenes, J.: Spatially distributed modeling: Conceptual approach, coupling surface water and ground-water, in Unsaturated Flow Hydrologic Modeling: Theory and Practice, NATO ASI Series C, vol. 275, edited by: Morel-Seytoux, H. J., 435–454, Kluwer Acad., Norwell, Mass, 1989.

Martin, E., Le Moigne, P., Masson, V., Boone, A., Bogatchev, A., Brut, A., Bouyssel, F., Calvet, J.-C., Champeaux, J.-L., Chancibault, K., Decharme, B., Donier, S., Douville, H., Dziedzic, A., Giard, D., Faroux, S., Fischer, C., Gibelin, A.-L., Habets, F., Hello, G., Jarlan, L., Kraljevic, L., Kullmann, L., Lac, C., Lacarrère, P., Lebeaupin, C., Mahfouf, J.-F., Malardel, S., Mallet, I., Marquet, P., Masson, V., Mokthar, M., Noilhan, J., Payart, J., Quintana-Seguí, P. Seity, Y., Tulet, P., Vincendon, B., Zaaboul, R., and Zuurendonk, I.: Le code de surface externalisé SURFEX de Météo-France, Ateliers de Modélisation de l'Atmosphère (http://www.cnrm.meteo.fr/ama2007/), Toulouse, 16–18 January, 2007.

Masson, V., Champeaux, J.-L., Chauvin, F., Meriguet, C., and Lacaze, R.: A global database of land surface parameters at 1-km resolution in meteorological and climate models, J. Climate, 16, 1261–1282, 2003.

Nakicenovic, N., Alcamo, J., Davis, G., de Vries, B., Fenhann, J., Gaffin, S., Gregory, K., Grübler, A., Jung, T., Kram, T., La Rovere, E., Michaelis, L., Mori, S., Morita, T., Pepper, W., Pitcher, H., Price, L., Riahi, K., Roehrl, A., Rogner, H.-H., Sankovski, A., Schlesinger, M., Shukla, P., Smith, S., Swart, R., van Rooijen, S., and Victor, N. Z. D.: IPCC Special Report on Emissions Scenarios. Cambridge University Press, Cambridge, United Kingdom and New York, NY, USA, 599 pp., 2000.

Noilhan, J. and Planton, S.: A simple parameterization of land surface processes for meteorological models, Mon. Weather Rev., 117, 536–549, 1989.

Noilhan, J. and Lacarrère, P.: GCM Grid-Scale Evaporation from Mesoscale Modeling, J. Climate, 8, 206–223, 1995.

Noilhan, J. and Mahfouf, J.-F.: The ISBA land surface parameterization scheme, Global Planet. Change, 13, 145–159, 1996.

Quintana Seguí, P., Le Moigne, P., Durand, Y., Martin, E., Habets, F., Baillon, M., Franchistéguy, L., Morel, S., and Noilhan, J.: Analysis of near-surface atmospheric variables: Validation of the SAFRAN analysis over France, J. Appl. Meteorol. Climatol., 47, 92–107, 2008.

Quintana Seguí, P., Ribes, A., Martin, E., Habets, F., and Boé, J.: Comparison of three downscaling methods in simulating the impact of climate change on the hydrology of Mediterranean basins, J. Hydrol., 383, 111–124, 2010.

Ritter, B. and Geleyn, J. F.: A comprehensive radiation scheme for numerical weather prediction models with potential applications in climate simulations, Mon. Weather Rev., 120, 303–325, 1992.

Sabater, J. M., Jarlan L., Calvet J.-C., Bouyssel F., and De Rosnay P.: From Near-Surface to Root-Zone Soil Moisture Using Different Assimilation Techniques, J. Hydrometeor., 8, 194–206, 2007.

Somot, S.: Modélisation climatique du bassin méditerranéen : variabilité et scénarios de changement climatique, Ph.D. thesis, Université Paul Sabatier, Toulouse, France, 2005.

Somot, S., Sevault, F., and Déqué, M.: Transient climate change scenario simulation of the Mediterranean Sea for the 21st century using a high resolution ocean circulation model, Clim. Dynam., 27, 851–879, 2006.

Somot, S., Sevault, F., Déqué, M., and Crepon, M.: 21st century climate change scenario for the Mediterranean using a coupled atmosphere-ocean regional climate model, Global Planet. Change, 63, 112–126, 2008.

van Pelt, S. C., Kabat, P., ter Maat, H. W., van den Hurk, B. J. J. M., and Weerts, A. H.: Discharge simulations performed with a hydrological model using bias corrected regional climate model input, Hydrol. Earth Syst. Sci., 13, 2387–2397, doi:10.5194/hess-13-2387-2009, 2009.

Welch, B. L.: The generalization of student's problem when several different population variances are involved, Biometrika, 34, 28–35, 1947.

Wood, A. W., Leung, L. R., Sridhar, V., and Lettenmaier, D. P.: Hydrologic implications of dynamical and statistical approaches to downscaling climate model outputs, Climat. Change., 62, 189–216, 2004.

Yang, W., Tan, B., Huang, D., Rautiniainen, M., Shabanov, N. V., and Wang, Y.: MODIS leaf area index products: From validation to algorithm improvement, IEEE T. Geosci Remote Sens., 44, 1885–1898, 2006.

Yin, X.: Responses of leaf nitrogen concentration and specific leaf area to atmospheric CO_2 enrichment: a retrospective synthesis across 62 species, Global Change Biol., 8, 631–642, 2002.